Metrol. Meas. Syst., Vol. XXII (2015), No. 3, pp. 443–454.

PAN POLSKA AKADEMIA NAUK

METROLOGY AND MEASUREMENT SYSTEMS
Index 330930, ISSN 0860-8229
www.metrology.pg.gda.pl

M&MS

APPLICATION OF KALMAN FILTER IN NAVIGATION PROCESS OF AUTOMATED GUIDED VEHICLES

Mirosław Śmieszek, Magdalena Dobrzańska

Rzeszów University of Technology, Faculty of Management, Al. Powstańców Warszawy 10, 35-959 Rzeszów, Poland
(✉ *msmieszk@prz.edu.pl*, +48 17 865 1602, *md@prz.edu.pl*)

Abstract

In the paper an example of application of the Kalman filtering in the navigation process of automatically guided vehicles was presented. The basis for determining the position of automatically guided vehicles is odometry – the navigation calculation. This method of determining the position of a vehicle is affected by many errors. In order to eliminate these errors, in modern vehicles additional systems to increase accuracy in determining the position of a vehicle are used. In the latest navigation systems during route and position adjustments the probabilistic methods are used. The most frequently applied are Kalman filters.

Keywords: Kalman filtering, odometry, laser measurements.

1. Introduction

To guide and determine the current position of an automated guided vehicle a variety of navigation systems are used which enable the vehicle to move from the starting point along a specified route to the destination. These systems while driving can use a real or virtual trajectory. In a navigation system with the real trajectory the vehicle is traveling on a closely-physically specified route. This route can be determined by means of an induction loop, or an optical or magnetic loop. In these three cases the devices fitted to the vehicle follow a designated route, and the vehicle control system strives to minimize the deviation between the position of the set route and the sensor or the camera.

In a navigation system which uses virtual trajectories the vehicle has its own advanced system with a sufficiently large memory. In the memory the map of the area and the route along which the vehicle is traveling are encoded. The control system uses data from the respective sensors and indicates the current position of the vehicle and other traffic parameters. The basis for determining the position in this type of navigation is odometry – the navigation calculation. This method of determining the vehicle position is affected by a number of errors. In order to eliminate these errors in modern vehicles additional systems are used – to increase the accuracy in determining the vehicle position [12, 21]. These systems include the optical, magnetic, laser and GPS satellite navigation [4, 7, 14, 18, 20, 24]. At appropriate time intervals, or after passing by the vehicle characteristic signs [11, 16, 23] there is a precise position determination process and error correction from the navigation computing – odometry. In the latest navigation systems in the process of the route and position adjustment the probabilistic methods are used. These methods are successfully used to analyse the measurement signals [5, 6, 13] and they have been quickly implemented in mobile robotics [11, 16].

Recently, extended Kalman filters have been widely applied [2, 9, 10]. Castellanos [2] have proposed application of an extended Kalman filter in an algorithm used for simultaneous mapping and location of a vehicle. It has been shown that linearization of resulting non-

Article history: received on Jan, 22, 2014; accepted on Jul. 03, 2015; available online in Sep. 21, 2015: DOI: 10.1515/mms-2015-0037.

linearities in both the motion of a vehicle and the sensor model enables to obtain good results in the applied algorithm.

2. An automated guided vehicle – the object of research

The object of research was an automatically guided vehicle designed to transport cargo, made at Rzeszów University of Technology. The vehicle motion was driven and controlled by two independently driving wheels. The tested facility was equipped with a computer, and a set of cards for data acquisition and control of an appropriate measurement equipment. Due to the lack of a flexible suspension the vehicle was designed to move on smooth surfaces. The vehicle was built based on the tricycle construction having two driving wheels and one wheel with independent rotation. Such a solution of high structural simplicity provides good manoeuvrability. The tested vehicle has the following dimensions: 1.24 x 1.04 m. In the vehicle MICROSONAR MS105 ultrasonic sensors and LT3 laser rangefinders have been applied. For the ultrasonic sensors settling time is 125 ms, repetition ±2 mm, and linearity ±8 mm. In contrast, for the laser rangefinders the settling time is 1; 10; 100 ms, linearity in the diffusion mode ±30 mm (0.3−1.5 m), ±20 mm (1.5−5.0 m), and in the reflective mode ±60 mm (0.5−50 m) [25, 26].

The basic method of calculating the position of an automated guided transport vehicle is the navigation calculation − odometry. It involves determining the current position of a vehicle, based on the distance travelled by the vehicle's characteristic point K. In practical solutions three methods of calculating navigation of a land vehicle are applied [15, 17]. These methods differ in a way of measuring and determining the azimuthal angle. In this research the navigation calculation was applied to determine the azimuthal angle θ and the difference in speeds of driving wheels v_L and v_P. The essence of this approach is shown in Fig. 1.

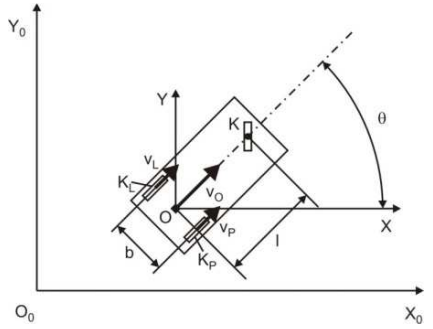

Fig. 1. The coordinate system adopted in the dead reckoning.

The applied method involves continuous calculating the distance travelled by the left (K_L) and right (K_P) wheels and determining in each of iterations the angle change θ of the directional movement of vehicle. The left and right wheels are coupled with encoders which generate 2000 pulses per one revolution of each wheel. The presented method is used in vehicles which need two independently driven driving wheels. The suitable differentiation of the rotational speed of these vehicles forces rotation of the vehicle around the vertical axis of rotation passing through the point O, and the direction angle change θ.

If the position of a chosen point O of the vehicle driven by two independent wheels of K_L and K_P in the base reference system $X_0O_0Y_0$ (Fig. 1) at the iteration k is determined by the state vector $\big(x(k), y(k), \theta(k)\big)$, then the position of the vehicle in the iteration $k + 1$ is expressed by the relation:

$$\begin{bmatrix} x(k+1) \\ y(k+1) \\ \theta(k+1) \end{bmatrix} = \begin{bmatrix} x(k) \\ y(k) \\ \theta(k) \end{bmatrix} + \begin{bmatrix} \Delta t \cdot v_{\mathrm{o}}(k+1) \cdot \cos\big(\theta(k) + \Delta t \cdot \omega(k+1)\big) \\ \Delta t \cdot v_{\mathrm{o}}(k+1) \cdot \sin\big(\theta(k) + \Delta t \cdot \omega(k+1)\big) \\ \Delta t \cdot \omega(k+1) \end{bmatrix}. \quad (1)$$

The speeds $v_{\mathrm{o}}(k+1)$ and $\omega(k+1)$ can be determined from the relations (2) and (3):

$$v_{\mathrm{O}}(k+1) = \big(v_{\mathrm{P}}(k+1) + v_{\mathrm{L}}(k+1)\big)/2, \quad (2)$$

$$\omega(k+1) = \big(v_{\mathrm{P}}(k+1) - v_{\mathrm{L}}(k+1)\big)/b, \quad (3)$$

where $v_{\mathrm{P}}(k+1)$ – the right wheel speed K$_{\mathrm{P}}$; $v_{\mathrm{L}}(k+1)$ – the left wheel speed K$_{\mathrm{L}}$; b – the driving wheel track.

The speeds $\boldsymbol{v_{\mathrm{P}}(k+1)}$ and $\boldsymbol{v_{\mathrm{L}}(k+1)}$ are expressed by the following relations:

$$v_{\mathrm{P}}(k+1) = \omega_{\mathrm{P}}(k+1) \cdot r, \quad (4)$$

$$v_{\mathrm{L}}(k+1) = \omega_{L}(k+1) \cdot r. \quad (5)$$

After taking into account the formulas (4) and (5) the angular velocity $\omega(k+1)$ (6) and the speed $v_{\mathrm{O}}(k+1)$ (7) can be obtained directly from the measurement of the angular velocity of the driving wheels $\omega_{\mathrm{P}}(k+1)$ and $\omega_{\mathrm{L}}(k+1)$:

$$\omega(k+1) = \big(\omega_{\mathrm{P}}(k+1) - \omega_{\mathrm{L}}(k+1)\big) \cdot r/b, \quad (6)$$

$$v_{\mathrm{O}}(k+1) = \big(\omega_{\mathrm{P}}(k+1) + \omega_{\mathrm{L}}(k+1)\big) \cdot r/2, \quad (7)$$

where $\omega_{\mathrm{P}}(k+1)$ – the angular speed of the right wheel; $\omega_{\mathrm{L}}(k+1)$ – the angular speed of the left wheel; r – the radius of the driving wheels which is the same for both wheels.

In the above discussion it was assumed that the wheels are rigid and roll without a slip, the wheel contact with the road is point-wise, and the radii r of the wheels are equal.

In a real vehicle there are a number of derogations from these assumptions. During the position determination the errors occur [3, 19, 22]. There are several sources of errors affecting the position accuracy. These sources are divided into two categories:

- Systematic errors caused by: an uneven distribution of the radii of the wheels, a bad connection of the wheels, an uncertainty in the track (due to a non-point wheel contact with the ground), a limited resolution of the encoder, a limited sampling rate of the encoder.
- Random errors caused by: driving over a rough surface, riding on random objects on the ground, slippage of the wheels (caused by a slippery ground, acceleration, fast curves (*i.e.*, skidding), external forces (interaction with external bodies), internal forces (wheel swivelling), a non-point wheel contact with the ground.

Systematic errors resulting from determination of the current position of a vehicle during movement are adding up, thus worsening the final result. At the most smooth surface indoor, the systematic errors have a greater share in the odometry errors than the random ones. However, on the surfaces with significant inequalities the random errors can be dominant.

In addition, the dead reckoning navigation errors may be caused by odometry equations as they approximate an arbitrary motion as a series of short straight sections. The accuracy of this approximation depends on the sampling frequency and the vehicle speed.

As the dominant sources of error in the odometry there are considered mainly the following ones:

- Different radii of the wheels – in the majority of automatically guided vehicles a mobile robot uses rubber-tyre wheels in order to improve adhesion and isolation from vibrations caused by an uneven work surface. It is very difficult to produce wheels of the same diameter. Moreover, rubber is deformed to different degrees, depending on the load and its asymmetrical distribution. Both of these cases are sources of odometry errors.

This error is marked as the radii error E_r:

$$E_r = \frac{r_L}{r_P}, \tag{8}$$

where r_L and r_P are the actual radii of the wheels.

– Uncertainties in the wheel track – the wheel track is defined as the distance between the points of contact where there is no slip in curvilinear motion of two wheels of the vehicle and the ground. The uncertainty in the track is caused by the fact that a pneumatic wheel is not in contact with the ground at a single point, but rather there is a space of contact. This error is marked as the track error E_b:

$$E_b = \frac{b_a}{b_n}, \tag{9}$$

where b_a – the current wheel track of the vehicle; b_n – the nominal wheel track of the vehicle.

The errors E_b and E_r are dimensionless quantities, expressed as fractions of the nominal value.

Not taking into account the above errors in the vehicle navigation results in a significantly rising deviation of distance from the given trajectory in time. This is evident in the graphs shown in Fig. 2.

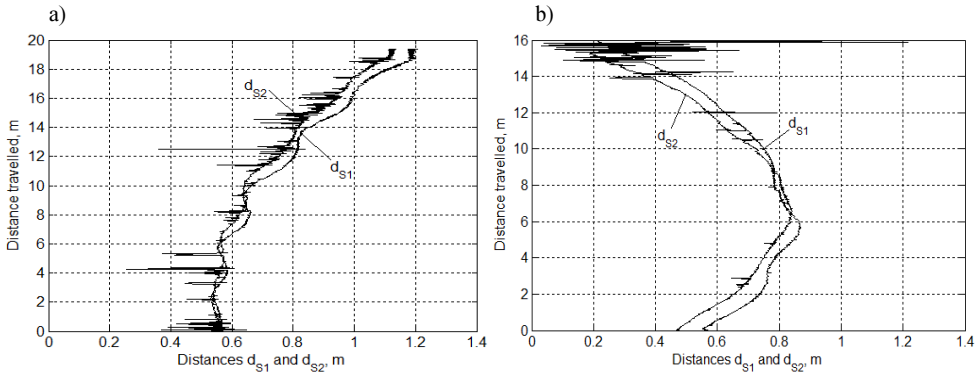

Fig. 2. The courses of two different samples determined on the basis of measurements from the sonars mounted on the front and rear of the vehicle.

The sonars S_1 and S_2 are located at the front and rear of vehicle and are engaged in continuous distance measurements of d_{S1} and d_{S2} from the wall of the corridor. The presented, measured actual course of motion is a curve and is close to an arc. This reflects the dominant role of errors in determining the wheel rolling radii. The recorded measurements are characterized by significant interference and thus the process requires appropriate filtering techniques. The need to ensure a high accuracy and measurement frequency eliminated the measurements with the use of a sonar. They were replaced by laser rangefinders.

Figure 3 shows examples of courses of driving along the wall. The vehicle control system based on measurement of data from a laser rangefinder tried to keep the vehicle at a predetermined distance from the wall. The courses in Fig. 3 are characterized by significant oscillations. This is caused by uneven walls, and interference of measurement results introduced into the control input.

In order to eliminate interference measurements it was necessary to apply a method of filtration of the obtained measurements. For this purpose, the most appropriate methodology seemed to be the Kalman filtering.

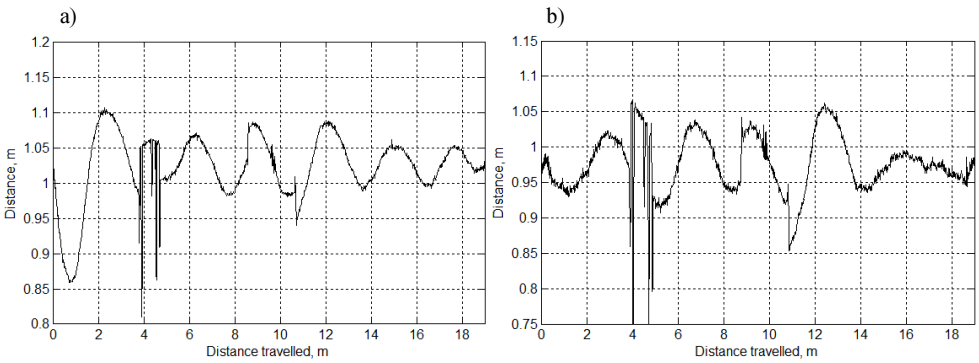

Fig. 3. The course of the vehicle determined based on data from a laser rangefinder for two different samples.

3. Methods of filtration – a Kalman filter

The absorption in the case of driving along the wall, the localization of an automated guided transport vehicle can be carried out by using probabilistic methods. It is based on estimation of a vector of the environment dynamic state based on sensory measurements. With respect to the automated guided vehicles, the state vector, for example, is formed by Cartesian coordinates of the centre of the vehicle and its orientation. The measurements are taken by odometry techniques and additionally by sensors, such as laser rangefinders, sonars and cameras. The key idea of probabilistic methods is recursive – at times k – estimation of the probability density in the whole state space, but providing the data received until the moment k. One of the probabilistic techniques of location of a mobile robot uses a Kalman filter [1]. During operation of the Kalman filter all the available information about the controlled system is processed in order to determine the interesting variables.

There is also included such information as the dynamics of the system and measuring devices, a statistical description of disturbances in the system, a description of the measurement errors, and information on the initial values of the determined variables. Its operation is based on prediction, for example, the current location of a vehicle, based on historical movements and ongoing environmental monitoring in such a way that the error is statistically minimized. The Kalman filter is used to track changes in the position and orientation of a vehicle with respect to a known location of the vehicle at the initial moment. To be able to use it the control system needs to have a model that can be written in the linear form, and disruption of the system must be of the Gaussian character.

In the case of the Kalman filter – also called minimally – mean square linear estimation [8] – a function of quality is minimized:

$$J = E\left[\left(\underline{\mathbf{x}} - \hat{\underline{\mathbf{x}}}\right)^T \cdot \left(\underline{\mathbf{x}} - \hat{\underline{\mathbf{x}}}\right)\right], \tag{10}$$

where $E[.]$ denotes the expected value in a statistical sense; $\hat{\underline{\mathbf{x}}}$ – the estimate $\underline{\mathbf{x}}$.

The mathematical model of the system takes the following form:

$$\begin{cases} \underline{\mathbf{x}}(k+1) = \mathbf{F}(k) \cdot \underline{\mathbf{x}}(k) + \underline{\mathbf{w}}(k), \text{ the process model} \\ \underline{\mathbf{z}}(k+1) = \mathbf{H}(k+1) \cdot \underline{\mathbf{x}}(k+1) + \underline{\mathbf{v}}(k+1), \text{ the measurement model} \end{cases} \tag{11}$$

This model consists of two equations that describe the observed process (object) and the measurement performed on it. We assume that the observed process is dynamic, *i.e.*, the vector $\underline{\mathbf{x}}$ changes at any time moment. The value of vector $\underline{\mathbf{x}}(k+1)$ at the next time point depends on:

- the current values of vector $\underline{\mathbf{x}}(k)$;
- the matrix $\mathbf{F}(k)$ associated with the process, which may also change over time;
- the current value of process noise $\underline{\mathbf{w}}(k)$.

There is no direct "access" to the variables of the $\underline{\mathbf{x}}$ process, one can only measure the linear combination $\underline{\mathbf{z}}$, defined by the measurement matrix $\mathbf{H}(k+1)$ which can also vary.

In the Kalman filter theory some assumptions are made:

- $\underline{\mathbf{w}}(k)$ – the process noise has zero mean value and is uncorrelated:

$$E\left[\underline{\mathbf{w}}(k)\right] = \mathbf{0},\ E\left[\underline{\mathbf{w}}(k)\underline{\mathbf{w}}^T(j)\right] = \mathbf{0},\ k \neq j, \tag{12}$$

- the noise auto-covariance matrix of the process $\mathbf{Q}(k)$ is positively definite and symmetric:

$$\mathbf{Q}(k) = E\left[\underline{\mathbf{w}}(k)\underline{\mathbf{w}}^T(k)\right], \tag{13}$$

- $\underline{\mathbf{v}}(k)$ – the measurement noise has zero mean value and is uncorrelated "with itself", and the noise of the process $\underline{\mathbf{w}}(k)$:

$$E\left[\underline{\mathbf{v}}(k)\right] = \mathbf{0},\ E\left[\underline{\mathbf{v}}(k)\underline{\mathbf{v}}^T(j)\right] = \mathbf{0},\ E\left[\underline{\mathbf{v}}(\mathrm{k})\underline{\mathbf{w}}^T(j)\right] = \mathbf{0},\ k \neq j, \tag{14}$$

- the noise auto-covariance matrix of the measurement $\mathbf{R}(k)$ is positively definite and symmetric:

$$\mathbf{R}(k) = E\left[\underline{\mathbf{v}}(\mathrm{k}) \cdot \underline{\mathbf{v}}^T(k)\right], \tag{15}$$

- the initial value of the process variable vector must satisfy the following conditions:

$$E\left[\underline{\mathbf{x}}(0)\right] = \underline{\mathbf{0}},\ E\left[\underline{\mathbf{x}}(0)\underline{\mathbf{x}}^T(0)\right] = \mathrm{P}_0,\ E\left[\underline{\mathbf{x}}(0)\underline{\mathbf{w}}^T(k)\right] = \mathbf{0},\ E\left[\underline{\mathbf{x}}(0)\underline{\mathbf{v}}^T(k)\right] = \mathbf{0}, \tag{16}$$

i.e., the auto-covariance function of the initial state should be known and the state cannot be correlated with neither the process nor the measurement noise.

Designations relevant for writing and understanding the Kalman filter operation:

$\hat{\underline{\mathbf{x}}}(k+1|k)$ – the vector forecast $\underline{\mathbf{x}}(k+1)$ based upon measurements $\underline{\mathbf{z}}(1), \ldots, \underline{\mathbf{z}}(k)$ (17)

$\hat{\underline{\mathbf{x}}}(k+1|k+1)$ – the vector estimator $\underline{\mathbf{x}}(k+1)$ based upon measurements $\underline{\mathbf{z}}(1), \ldots, \underline{\mathbf{z}}(k+1)$ (18)

$\hat{\underline{\mathbf{z}}}(k+1|k)$ – the vector forecast $\underline{\mathbf{z}}(k+1)$ based upon measurements $\underline{\mathbf{z}}(1), \ldots, \underline{\mathbf{z}}(k)$ (19)

$$\Delta\underline{\mathbf{x}}(k|k) = \underline{\mathbf{x}}(k) - \hat{\underline{\mathbf{x}}}(k|k) \text{ – the state process estimation error,} \tag{20}$$

$$\Delta\underline{\mathbf{x}}(k+1|k) = \underline{\mathbf{x}}(k+1) - \hat{\underline{\mathbf{x}}}(k+1|k) \text{ – the state process forecast error,} \tag{21}$$

$$\Delta\underline{\mathbf{z}}(k+1|k) = \underline{\mathbf{z}}(k+1) - \hat{\underline{\mathbf{z}}}(k+1|k) \text{ – the measurement forecast error,} \tag{22}$$

$\mathbf{P}(k|k) = E\left[\Delta\underline{\mathbf{x}}(k|k)\Delta\underline{\mathbf{x}}^T(k|k)\right]$ – the covariance matrix of state process estimation error (23)

$\mathbf{P}(k+1|k) = E\left[\Delta\underline{\mathbf{x}}(k+1|k)\Delta\underline{\mathbf{x}}^T(k+1|k)\right]$ – the covariance matrix of state process forecast error, (24)

$\mathbf{P}(k+1|k+1) = E\left[\Delta\underline{\mathbf{x}}(k+1|k+1)\Delta\underline{\mathbf{x}}^T(k+1|k+1)\right]$ – the covariance matrix of object's status estimator error. (25)

The calculation scheme is shown in Fig. 4, whereas a block diagram of the Kalman filter in Fig. 5.

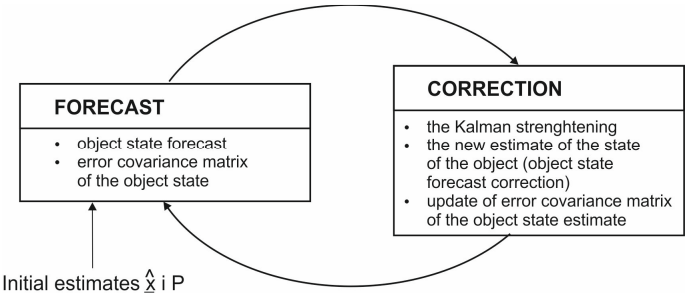

Fig. 4. The scheme of calculations of the Kalman filter algorithm.

Because the object is dynamically changeable, the forecast of the new state is not equal to the estimation of the previous state, but it is calculated taking into account the matrix of process "dynamics" **F** [8]. The Kalman filter algorithm may be used to identify parameters of a dynamic linear system and to "de-interleaving" signals, that is to estimate one of the intertwining signals with each other, based on knowledge of the second signal and a result of convolution. A result of passing the signal through the linear system line is its convolution with the impulse response of this system, thus often in practice it occurs a problem for adaptive estimation of the input signal based on knowledge of the "output" of the system and its transfer function.

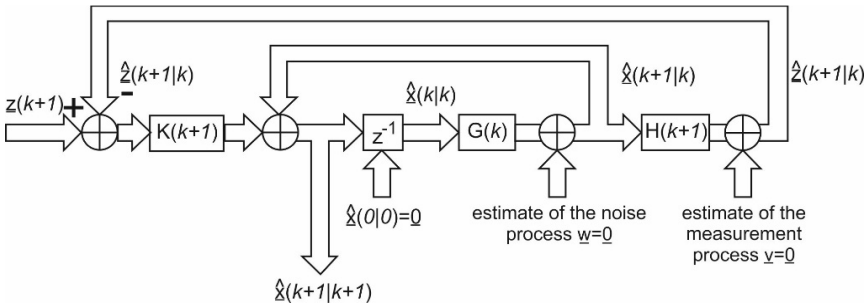

Fig. 5. A block diagram of the Kalman filter.

The task of Kalman filtering is to find the best linear estimate of minimally – mean squared vector $\underline{\mathbf{x}}(k)$ based on the values of the measurements done so far $\underline{\mathbf{z}}(i), i = 1, 2, 3, \ldots, k$. Since the noise $\underline{\mathbf{w}}(k)$ is not correlated with the measurements $\underline{\mathbf{z}}(i), i = 1, 2, 3, \ldots, k$, thus:

$$\hat{\underline{\mathbf{w}}}(k|k) = \mathbf{0}, \tag{26}$$

$$\hat{\underline{\mathbf{x}}}(k+1|k) = \mathbf{F}(k) \cdot \hat{\underline{\mathbf{x}}}(k|k) + \hat{\underline{\mathbf{w}}}(k|k) = \mathbf{F}(k) \cdot \hat{\underline{\mathbf{x}}}(k|k). \tag{27}$$

Similarly, because the noise $\underline{\mathbf{v}}(k)$ is not correlated with the measurements $\underline{\mathbf{z}}(j)$for $k \neq j$, hence:

$$\hat{\underline{\mathbf{v}}}(k+1|k) = \mathbf{0}, \tag{28}$$

$$\hat{\underline{\mathbf{z}}}(k+1|k) = \mathbf{H}(k+1) \cdot \hat{\underline{\mathbf{x}}}(k+1|k) + \hat{\underline{\mathbf{v}}}(k+1|k) = \mathbf{H}(k+1) \cdot \hat{\underline{\mathbf{x}}}(k+1|k). \tag{29}$$

The new estimate $\hat{\underline{\mathbf{x}}}(k+1|k+1)$ should be made up of the sum of two independent estimates:

$$\hat{\underline{\mathbf{x}}}(k+1|k+1) = \hat{\underline{\mathbf{x}}}(k+1|k) + \hat{\underline{\mathbf{x}}}\left(k+1 \middle| \underline{\Delta \mathbf{z}}(k+1|k)\right), \tag{30}$$

where the second summand of the sum means the component of the estimate $\hat{\underline{\mathbf{x}}}(k+1|k+1)$ based only on the forecast error of the $(k+1)$ st measurement.

The minimally-mean squared estimate of the vector $\underline{\mathbf{x}}$ based on the mean $\underline{\mathbf{z}}$ is equal to:

$$\hat{\underline{\mathbf{x}}} = \mathbf{G}\underline{\mathbf{z}},\ \mathbf{G} = \mathbf{R}_{\underline{\mathbf{x}}\,\underline{\mathbf{z}}}\mathbf{R}_{\underline{\mathbf{z}}\,\underline{\mathbf{z}}}^{-1},\ \mathbf{R}_{\underline{\mathbf{x}}\,\underline{\mathbf{z}}} = E\left[\underline{\mathbf{x}}\,\underline{\mathbf{z}}^T\right],\ \mathbf{R}_{\underline{\mathbf{z}}\,\underline{\mathbf{z}}} = E\left[\underline{\mathbf{z}}\,\underline{\mathbf{z}}^T\right], \tag{31}$$

because its error must be orthogonal to the vector of $\underline{\mathbf{z}}$ measurements:

$$E\left[\underline{\mathbf{e}}\,\underline{\mathbf{z}}^T\right] = E\left[\left(\underline{\mathbf{x}} - \hat{\underline{\mathbf{x}}}\right)\underline{\mathbf{z}}^T\right] = E\left[\left(\underline{\mathbf{x}} - \mathbf{G}\underline{\mathbf{z}}\right)\underline{\mathbf{z}}^T\right] = E\left[\underline{\mathbf{x}}\,\underline{\mathbf{z}}^T\right] - \mathbf{G}E\left[\underline{\mathbf{z}}\,\underline{\mathbf{z}}^T\right] = \mathbf{R}_{\underline{\mathbf{x}}\,\underline{\mathbf{z}}} - \mathbf{G}\mathbf{R}_{\underline{\mathbf{z}}\,\underline{\mathbf{z}}} = 0, \tag{32}$$

After taking into account the (31) with respect to the second component of the sum of (30) we obtain:

我觉得此处有错误

$$\hat{\underline{\mathbf{x}}}\left(k+1\middle|\underline{\Delta\mathbf{z}}(k+1|k)\right) = \mathbf{K}(k+1)\cdot\underline{\Delta\mathbf{z}}(k+1|k), \tag{33}$$

$$\mathbf{K}(k+1) = E\left[\underline{\mathbf{x}}(k+1)\cdot\underline{\Delta\mathbf{z}}^T(k+1|k)\right]\cdot\left\{E\left[\underline{\Delta\mathbf{z}}(k+1|k)\underline{\Delta\mathbf{z}}^T(k+1|k)\right]\right\}^{-1}, \tag{34}$$

After the transformation, the relation (34) can be written in the following form:

$$\mathbf{K}(k+1) = [\mathbf{P}(k+1|k)\mathbf{H}^T(k+1)]\cdot[\mathbf{H}(k+1)\mathbf{P}(k+1|k)\mathbf{H}^T(k+1) + \mathbf{R}(k+1)]^{-1}, \tag{35}$$

where:

$$\mathbf{P}(k|k) = E\left[\underline{\Delta\mathbf{x}}(k|k)\cdot\underline{\Delta\mathbf{x}}^T(k|k)\right], \tag{36}$$

$$\mathbf{P}(k+1|k) = E\left[\underline{\Delta\mathbf{x}}(k+1|k)\underline{\Delta\mathbf{x}}^T(k+1|k)\right] = \mathbf{F}(k)\mathbf{P}(k|k)\mathbf{F}^T(k) + \mathbf{Q}(k), \tag{37}$$

$$\mathbf{P}(k+1|k+1) = E\left[\underline{\Delta\mathbf{x}}(k+1|k+1)\underline{\Delta\mathbf{x}}^T(k+1|k+1)\right] = [\mathbf{I} - \mathbf{K}(k+1)\mathbf{H}(k+1)]\cdot\mathbf{P}(k+1|k). \tag{38}$$

The transformations from the (34) into the (35) take into account the definitions and (11), (13), (15), (21), (22), (27) and (29), and the property "uncorrelation" ("orthogonality") of the vector pairs $\left\{\underline{\Delta\mathbf{x}}(k+1|k), \underline{\mathbf{w}}(k+1)\right\}$ and $\left\{\underline{\Delta\mathbf{x}}(k+1|k), \underline{\mathbf{v}}(k+1)\right\}$:

$$E\left[\underline{\Delta\mathbf{x}}(k+1|k)\underline{\mathbf{w}}^T(k+1)\right] = 0,\ E\left[\underline{\Delta\mathbf{x}}(k+1|k)\underline{\mathbf{v}}^T(k+1)\right] = 0. \tag{39}$$

The methodology previously described has been implemented in a computer program controlling the movement of the vehicle in real time.

4. Analysis of the results

Experimental studies with the use of laser rangefinders have been divided into two stages: the preliminary stage and the basic research one. Within the preliminary studies the measurements verifying the methods and measurement systems were performed. Firstly, the scatter measurements obtained from a laser rangefinder were determined. For this purpose, the measurements were made with a stationary laser rangefinder located on a rigid substrate, and then with the laser rangefinder located on the vehicle with working propulsion engines.

In Fig. 6 the benefits of using the Kalman filtering are shown. Fig. 6a shows the course of the recorded and processed signal from the laser rangefinder mounted on a rigid surface. Noticeable scattering of measurements is about 2 mm, which is approximately 1‰ of the measured range. Fig. 6b shows the course obtained from the measurement using the laser rangefinder located on the vehicle. The wheels of the vehicle during the measurement were raised, whereas the motor drives were working and lifted vehicle vibrations. The black line maps the obtained results. The resulting dispersion in measurements is much larger, as shown in Fig. 6a. During the measurement the obtained results were subjected to filtration through a

real-time Kalman filter. The effects of the filter are shown in Fig. 6b as the white line. Scattering of the measurement results after filtration is largely limited.

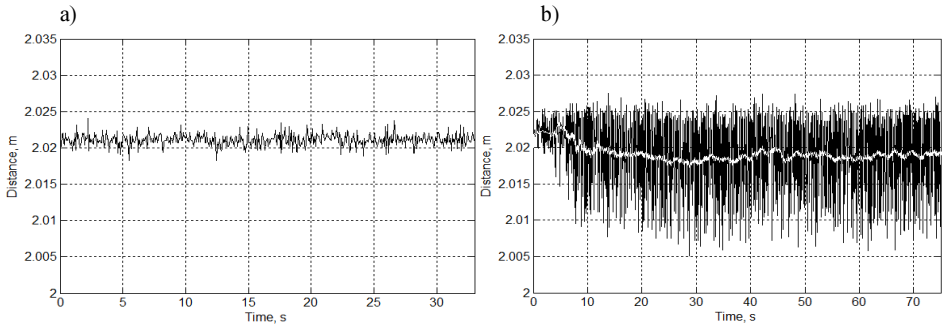

Fig. 6. The course diagrams of the measured distance by a laser rangefinder located: a) (disassembled from the vehicle) on a rigid substrate; b) on the vehicle with working propulsion engines; the white line on the diagram is the course after the Kalman filtering.

The Kalman filter used a vehicle model built specially for this purpose. The state vector consisted of the Cartesian coordinates of the centre of the vehicle, its orientation, the radii of the wheels and the wheel track. The state vector has been described by the (40). The measurements were made with the odometry techniques using sensors, such as laser rangefinders.

$$\begin{bmatrix} x_1 \\ x_2 \\ x_3 \\ x_4 \\ x_5 \\ x_6 \end{bmatrix} = \begin{bmatrix} x \\ y \\ \theta \\ r_L \\ r_P \\ b \end{bmatrix}. \tag{40}$$

The sizes of x_1, x_2, x_3 are described by the (1) whereas x_4, x_5, x_6 by the relations (41).

$$\begin{aligned} x_4(k+1) &= x_4(k), \\ x_5(k+1) &= x_5(k), \\ x_6(k+1) &= x_6(k), \end{aligned} \tag{41}$$

At the second stage of the performed tests the vehicle was at a predetermined distance from the base surface on the basis of measurements of the laser rangefinder subjected to the Kalman filtering. The measurements of the laser rangefinder were used by the control system to drive at a constant distance from the base surface.

The filtration process requires estimation of the variance of process and measurement. The value of the measurement variance has been determined on the basis of catalogue data and preliminary stationary measurements. To determine the value of the process variance the reference data have been applied. During the experiments, these values have been changed several times.

To better illustrate the impact of the Kalman filtering, in Fig. 7 a small part of the route with visible courses of the measurement data before and after filtration was shown.

In Fig. 8a there are presented the courses of the vehicle's distances from the wall obtained from the indications of the laser rangefinder without filtration, and Fig. 8b shows the distance from the wall based on the indications obtained from the laser rangefinder subjected to Kalman filtering.

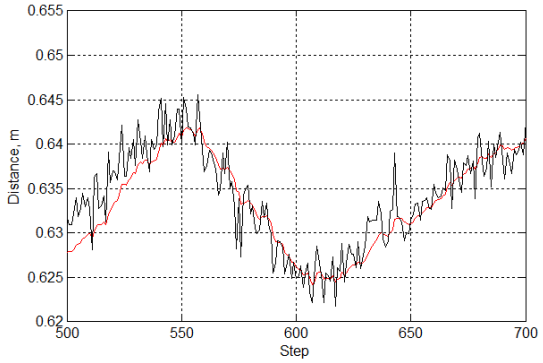

Fig. 7. A selected portion of the course in linear motion; the black line – the course before filtration, the red line – the course subjected to filtering.

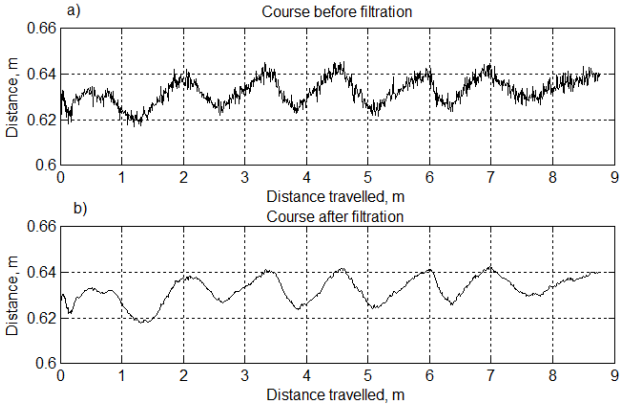

Fig. 8. The course of the vehicle determined on the basis of data from the laser rangefinder: a) before filtration; b) after filtration.

To demonstrate the influence of filtering the measurement signals on the vehicle motion in Figs. 3 and 9 there were shown the courses obtained from the vehicle using the unfiltered and filtered measurement signals. When comparing the courses from Fig. 3 (without filtration) and Fig. 9 (with filtration) it can be concluded that the use of the Kalman filtering significantly reduces oscillations of the vehicle along the implemented route.

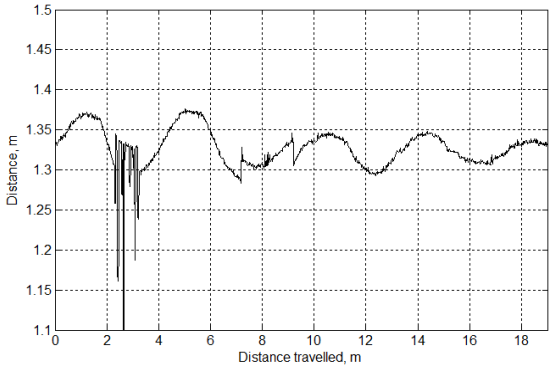

Fig. 9. The distance from the base surface obtained from the measurements of the laser after filtration when the vehicle is travelling.

In both considered cases, the maximum oscillations are observed when the vehicle passes through an obstacle disturbing the measurement. In the case of the Kalman filter the maximum size of the oscillation is less than about 30% in comparison to that obtained without filtration, and is quickly stabilized. The final value of these oscillations is also lower. The standard deviation for the considered phase of movement after passing a measurement obstacle for the unfiltered course is 0.0297 whereas for the filtered one is only 0.0189.

5. Conclusions

Contemporary measurement techniques enable measurements with a considerable accuracy and frequency. In a real research facility such as a vehicle we have to deal with vibrations from the road and the drive unit. The shape and profile of the measured items in many cases are characterized by significant deviations. In spite of a high accuracy of measurement devices a series of disturbances is imposed on the obtained results, which in turn makes it impossible to precisely determine the position and driving along a specified route. The disturbances are random; therefore, a very good solution is to use the Kalman filtering. The performed studies showed clearly the benefits of such a solution. This is seen by comparing the graphs in Figs. 3 and 9. The use of the Kalman filter resulted in a significant reduction in deviation from the specified route. The vehicle movement became smoother and enabled an early indication of other very important quantities for the process of navigation, such as the ratio of the rolling radii.

References

[1] Bong-Su, Ch., Woo-Sung, M., Woo-Jin, S., Kwang-Ryul, B. (2011). A dead reckoning localization system for mobile robots using inertial sensors and wheel revolution encoding. *Journal of Mechanical Science and Technology*, 25(11), 2907–2917.

[2] Castellanos, J.A., Martinez-Cantin, R., Tardós, J.D., Neira, J. (2007). Robocentric map joining: Improving the consistency of EKF-SLAM. *Robotics and Autonomous Systems*, 55, 21–29.

[3] Changbae, J., Chang-Bae, M., Daun, J., Jong-Suk, Ch., Woojin, Ch. (2014). Design of Test Track for Accurate Calibration of Two Wheel Differential Mobile Robots. *International Journal of Precision Engineering and Manufacturing*, 15(1), 53–61.

[4] Diosi, A., Kleeman, L. (2004). Advanced sonar and laser range finder fusion for simultaneous localization and mapping. *Proc. of 2004 IEEE/RSJ International Conference on Intelligent Robots and Systems*, Sendai Japan, 1854–1859.

[5] Dobrzanski, P., Pawlus, P. (2010). Digital filtering of surface topography: Part: I. Separation of one-process surface roughness and waviness by Gaussian convolution, Gaussian regression and spline filters. *Precision Engineering-Journal of the International Societies for Precision Engineering and Nanotechnology*, 34(3), 647–650.

[6] Dobrzanski, P., Pawlus, P. (2010). Digital filtering of surface topography: Part II. Applications of robust and valley suppression filters. *Precision Engineering-Journal of the International Societies for Precision Engineering and Nanotechnology*, 34(3), 651–658.

[7] Epton, T., Hoover, A. (2012). Improving odometry using a controlled point laser. *Autonomous Robots*, 32, 165–172.

[8] Grewal, M.S., Andrews, A.P. (2008). *Kalman Filtering: Theory and Practice with MATLAB*. Wiley.

[9] Joerger, M., Pervan, B. (2013). Kalman Filter-Based Integrity Monitoring Against Sensor Faults. *Journal of Guidance Control and Dynamics*, 36(2), 349–361.

[10] Joerger, M., Pervan, B. (2009). Measurement-level integration of carrier-phase GPS and laser-scanner for outdoor ground vehicle navigation. *Journal of Dynamic Systems, Measurement, and Control*, 131/021004-1–021004-11.

[11] Jung-Suk, L., Wan Kyun, Ch. (2010). Robust mobile robot localization in highly non-static environments. *Autonomous Robots*, 29, 1–16.

[12] Jungmin, K., Seungbeom, W., Jaeyong, K., Joocheol, D., Sungshin, K., Sunil, B. (2012). Inertial Navigation System for an Automatic Guided Vehicle with Mecanum Wheels. *International Journal of Precision Engineering and Manufacturing*, 13(3), 379–386.

[13] Kaplonek, W., Łukianowicz, Cz., Nadolny, K. (2012). Methodology of the assessment of the abrasive tool's active surface using laser scatterometry. *Transactions of the Canadian Society for Mechanical Engineering*, 36(1), 49–66.

[14] Kasinski, A., Skrzypczynski, P. (2001). Perception network for the team of indoor mobile robots: concept, architecture, implementation. *Engineering Applications of Artificial Intelligence*, 14, 125–137.

[15] Kelly, A. (2004). Linearized error propagation in odometry. *International Journal of Robotics Research*, 23(2), 179–218.

[16] Knuth, J., Barooah, P. (2013). Error growth in position estimation from noisy relative pose measurements. *Robotics and Autonomous Systems*, 61, 229–244.

[17] Kooktae, L., Changbae, J., Woojin, Ch. (2011). Accurate calibration of kinematic parameters for two wheel differential mobile robots. *Journal of Mechanical Science and Technology*, 25(6), 1603–1611.

[18] Madhavan, R., Durrant-Whyte, H.F. (2004). Terrain-aided localization of autonomous ground vehicles. *Automation in Construction*, 13, 83–100.

[19] Martinelli, A., Tomatis, N., Siegwart, R. (2007). Simultaneous localization and odometry self-calibration for mobile robot. *Autonomous Robots*, 75–85.

[20] Pears, N.E. (2000). Feature extraction and tracking for scanning range sensors. *Robotics and Autonomous Systems*, 33, 43–58.

[21] Roberts, J.M., Duff, E.S., Corke, P.I. (2002). Reactive navigation and opportunistic localization for autonomous underground mining vehicles. *Information Sciences*, 145, 127–146.

[22] Shoval, S., Zeitoun, I., Lenz, E. (1997). Implementation of a Kalman Filter in positioning for autonomous vehicles, and its sensitivity to the process parameters. *International Journal of Advanced Manufacturing Technology*, 738–746.

[23] Smieszek, M., Dobrzanska, M., Dobrzanski, P. (2010). Errors in odometry navigation. *ICMEM, HLOCH,* Presov, 124–128.

[24] Tungadi, F., Kleeman, L. (2011). Discovering and restoring changes in object positions using an autonomous robot with laser rangefinders. *Robotics and Autonomous Systems* 59, 428–443.

[25] *www.nivelco.pl* (Dec. 2014).

[26] *www.turck.pl* (Dec. 2014).